CHEM / BCMB 4190/6190/8189

Introductory NMR

Lecture 11

Spin-Echo

<u>The spin-echo pulse sequence:</u> 90˚x' - τ - 180˚x' - τ(echo)

- **Spins echoes are widely used as part of larger pulse sequence to refocus the effects of:**
  - **1) unwanted chemical shift precession**
  - **2) magnet inhomogeneity**
  - **3) heteronuclear J coupling**
- **The spin-echo does not refocus homonuclear J coupling**
- **The spin-echo pulse sequence can be used to measure the relaxation parameterT_2 ; it does not refocus the effect of T_2 relaxation**

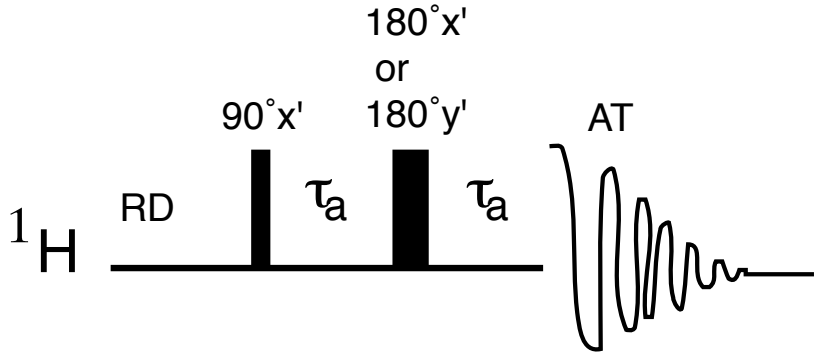

Typical delays and pulse lengths:

RD = Recycling delay ~ 1 sec.
τ_a = Spin-echo delay ~ 50 ms
AT = Acquisition time ~ 0.2 sec.
90˚ ~ 10 μs
180˚ ~ 20 μs

The spin-echo in vector diagram

A) Lets consider the non-coupled single spin case.
Example: ^{1}H in $CHCl_3$ (carbon not ^{13}C-labeled)
with $\nu_H = \nu_{rf} + 100$ Hz

^{1}H: 90˚x- τa - 180˚y - τa (echo)

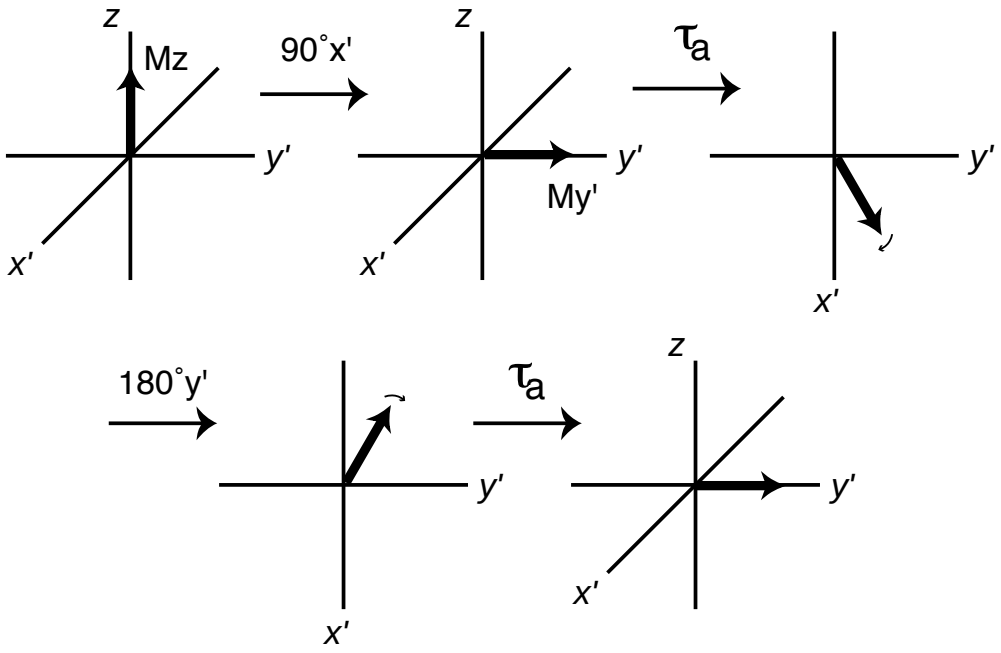

Detected Signal after FT:

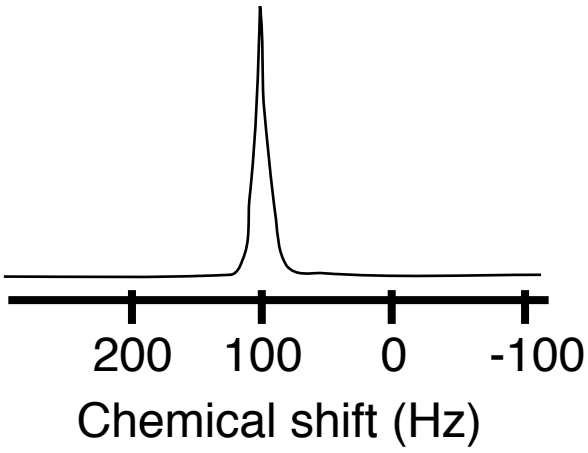

^{1}H: 90˚x- τa - 180˚x - τa (echo)

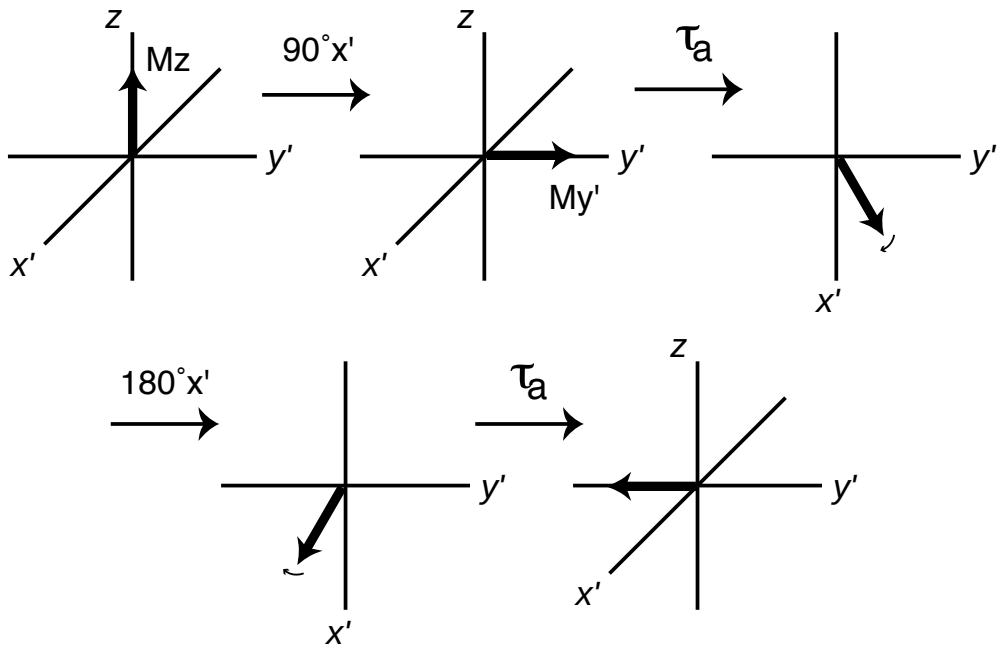

Detected Signal after FT:

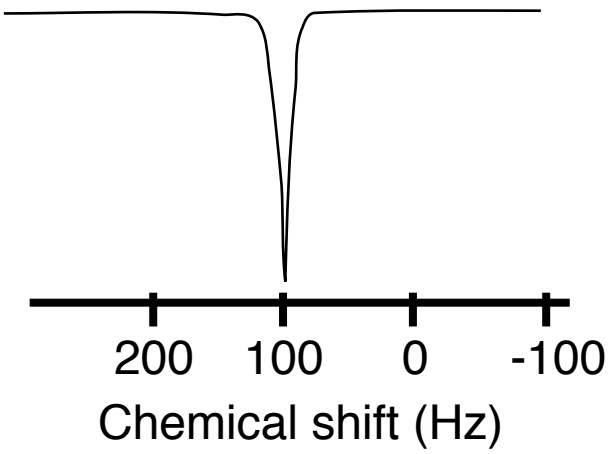

Note that the intensity is ploted relatively to the positive signal on the previous page. In practice, this signal would be drawn as a positive signal by adjusting the zero order phase correction by 180˚.

<u>Conclusions</u>:

1) Chemical shift evolution (precession) is refocused by the spin-echo

2) Similarly the spin-echo refocuses magnet inhomogeneity (ΔB_o):

- **The magnetic field B_o is not perfectly homogeneous throughout the volume of the sample, therefore not all nuclei experience the same magnetic field.**
- **The small differences in magnetic field (ΔB_o) across the sample volume causes nuclei that are chemically equivalent to precess at different rate.**

B) Lets consider a simple case of heteronuclear coupling, i.e. a two-spin AX system with A = ^{1}H and X = ^{13}C
Example: ^{13}C in $CHCl_3$ (carbon is ^{13}C-labeled) with $\nu_{rf} = \nu_H$
$^{1}J_{AX}$ = 209 Hz

^{13}C: 90˚x- τa - 180˚x - τa (echo)- Acquisition time

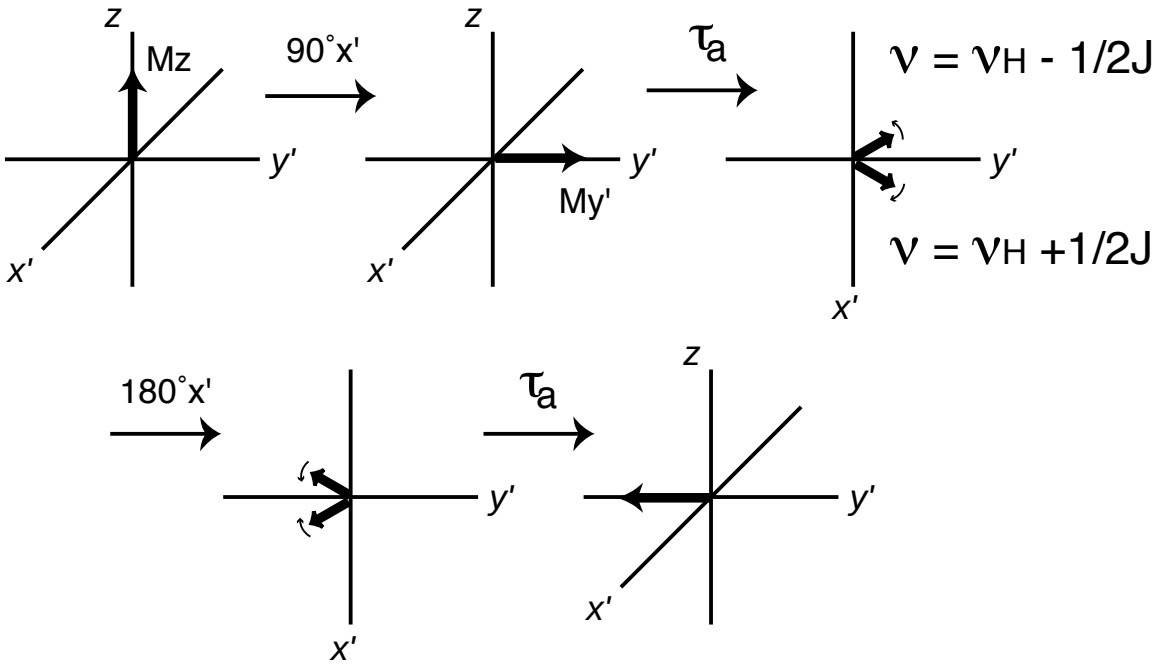

Detected Signal after FT:

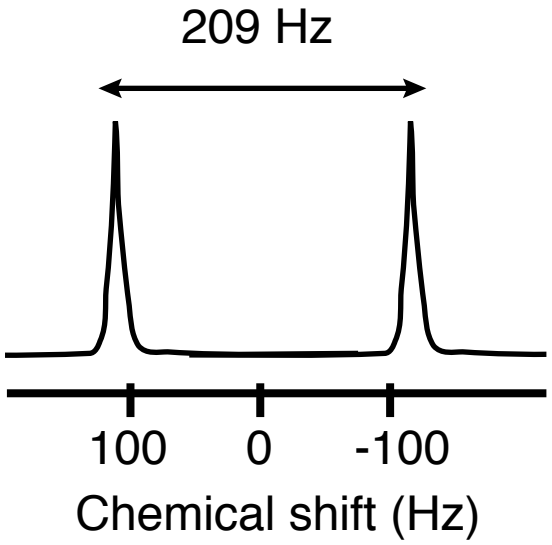

More on the two-spin AX system with A=^{1}H and X=^{13}C (e.g. ^{13}CHCl3):

1) Energy level diagram

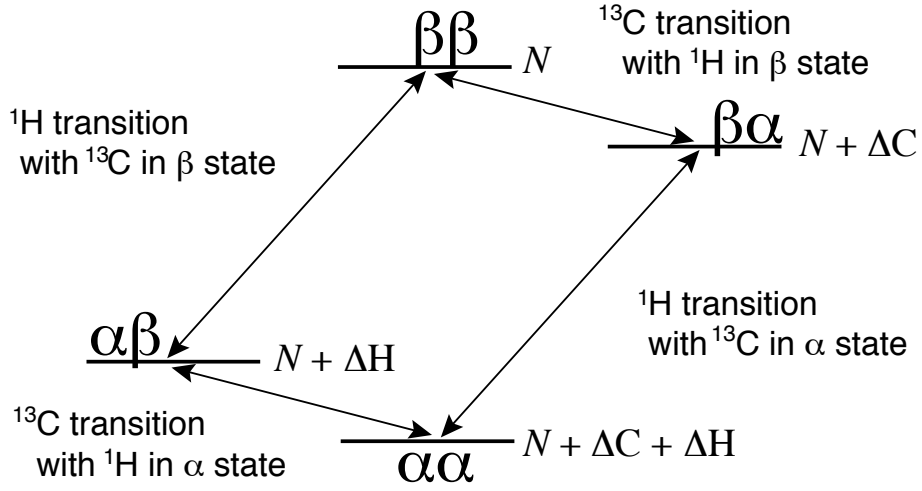

2) Essentially equal population differences for the ^{13}C transitions for ^{13}CHαCl3 and ^{13}CHβCl3

Population diferences:

αα to αβ transition: (*N* + ΔH + ΔC) - (*N* + ΔH) = ΔC
βα to ββ transition: (*N* + ΔC) - (*N*) = ΔC
αα to βα transition: (*N* + ΔH + ΔC) - (*N* + ΔC) = ΔH
αβ to ββ transition: (*N* + ΔH) - (*N*) = ΔH

3) Two different Larmor frequencies as a result of C-H coupling

ν (^{13}CHαCl3) = νc - 1/2*JCH
ν (^{13}CHβCl3) = νc + 1/2*JCH

with JCH = 209 Hz and δ = 77.7 ppm (center of the doublet)

4) In the first delay τ of the spin-echo experiment, a phase angle Θ is created between these two vectors

Θ = 2πJCH* τ

Examples: If τ = 0 than Θ = 0, if τ = 1/(4J) than Θ = π/2 = 90˚, etc.

Pulse sequence of the ‚J-modulated spin-echo experiment:

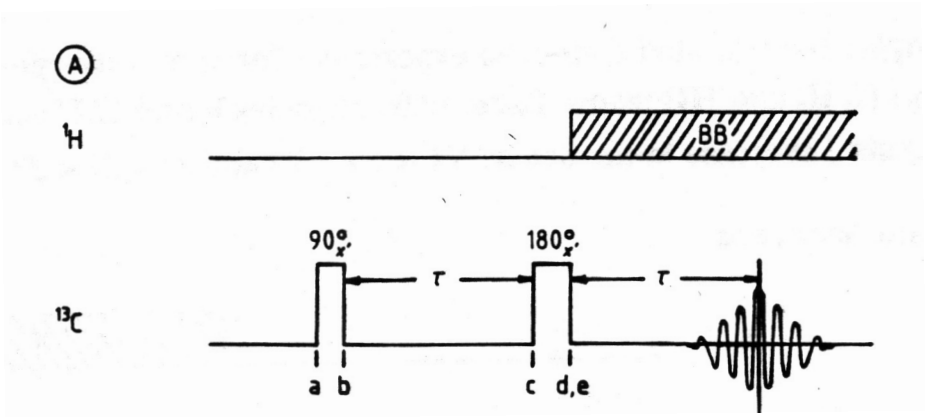

Vector diagrams for the ‚J-modulated spin-echo experiment:

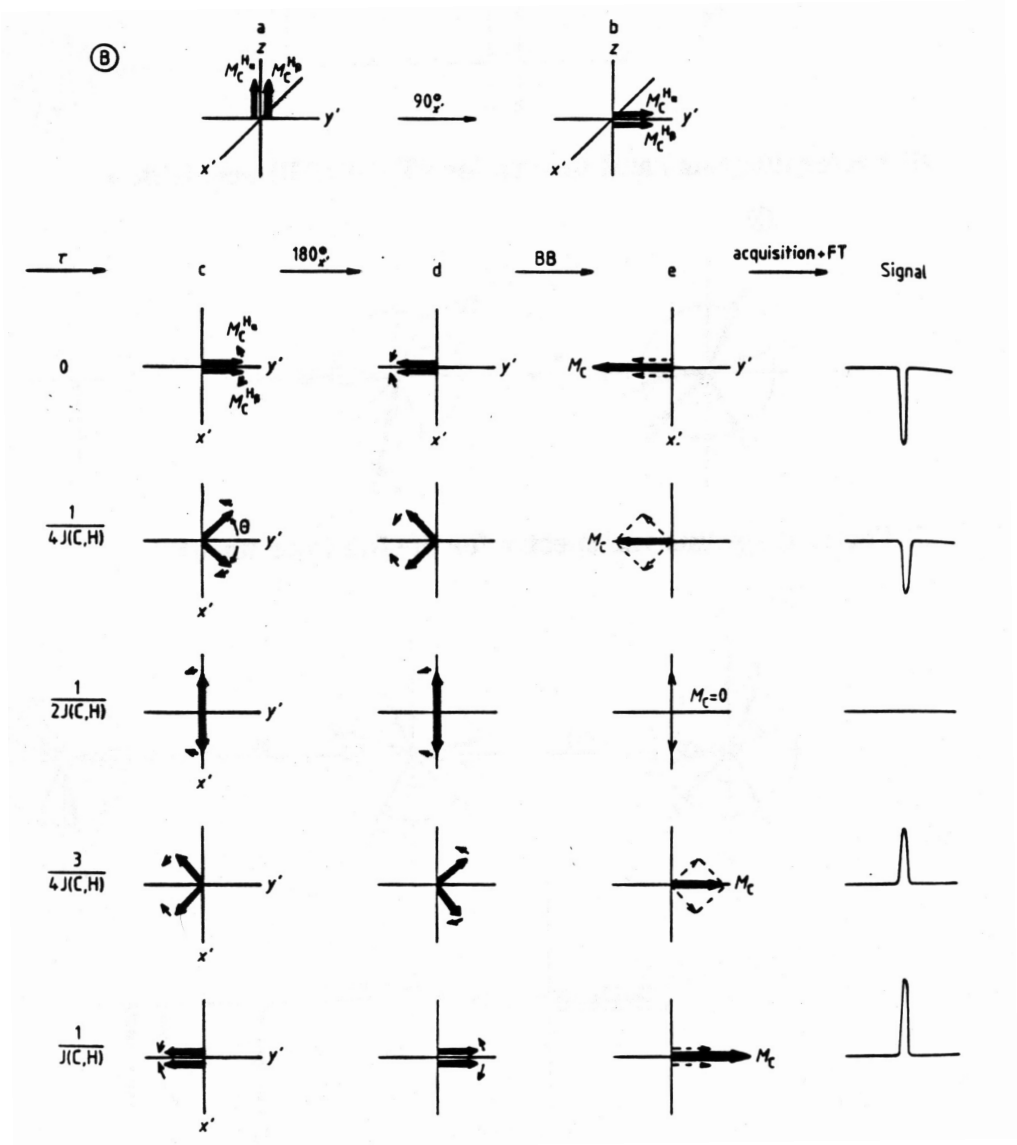

<u>Chemical-shift refocusing in the J-modulated spin-echo experiment</u>:

Example: J-modulated spin-echo experiment for three different CH groups (I, II, and III) whose Larmor frequencies ν and C-H coupling constants J increase in the order: $\nu_1 < \nu_2 < \nu_3$ and $J_1 < J_3 < J_2$

A) Pulse sequence

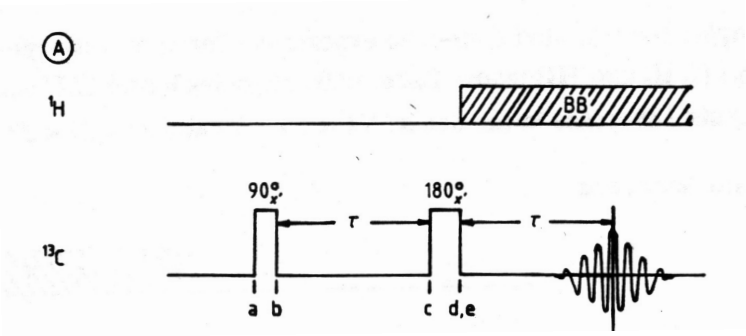

B) Vector diagrams and spectra for 90°x'-τ (BB)-acquisition

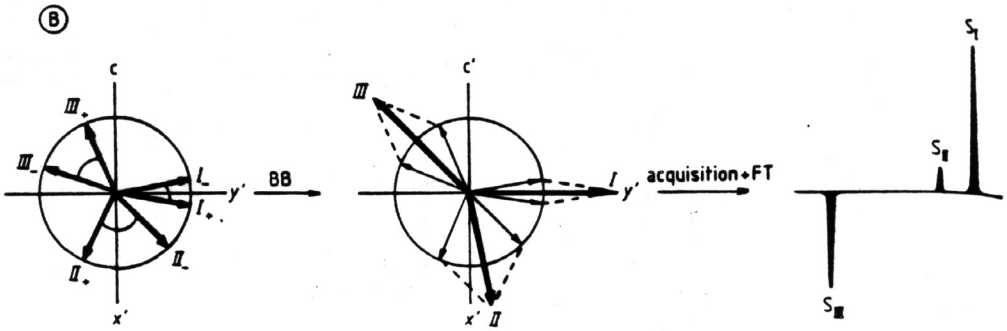

C) Vector diagrams and spectra for the full experiment

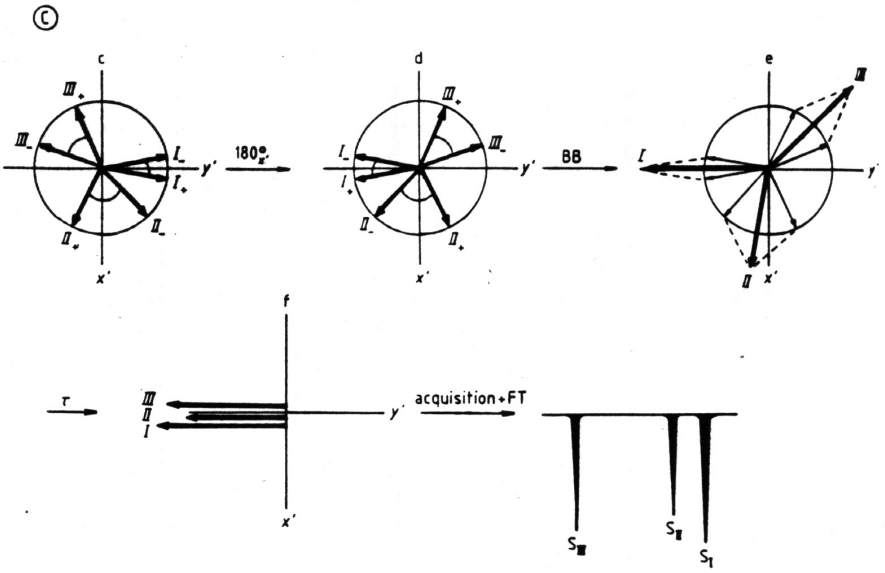

<u>Attached proton test (APT) with the J-modulated experiment</u>:

Lets consider various types of carbons and their precession frequencies:

- **quaternary carbon (Cq):** νc
- **CH group:** $\nu c \pm 1/2 * J_{CH}$
- **CH_2 group:** $\nu c, \nu c \pm J_{CH}$
- **CH_3 group:** $\nu c \pm 1/2 * J_{CH}, \nu c \pm 3/2 * J_{CH}$

Pulse sequence and vector diagram:

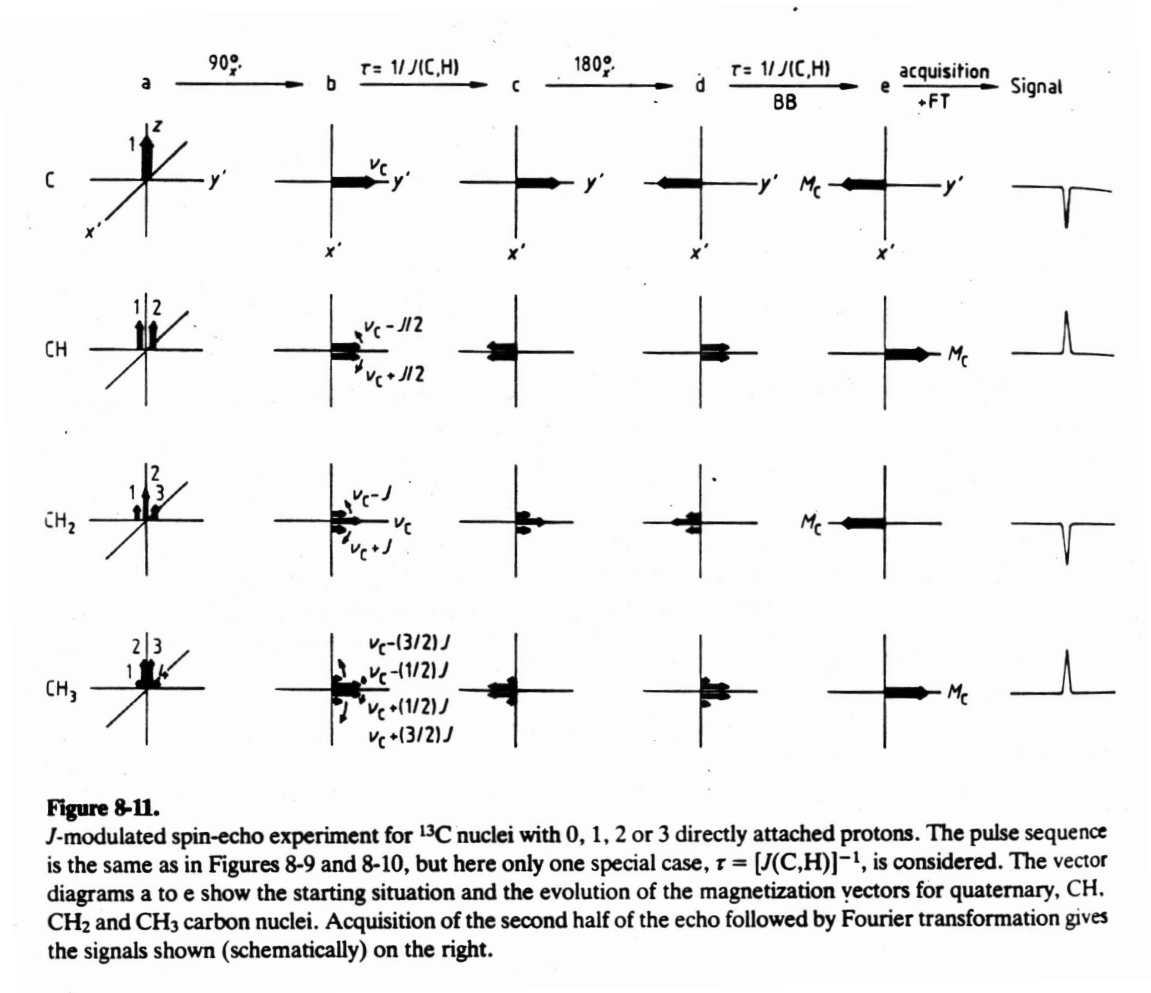

Figure 8-11.
J-modulated spin-echo experiment for ^{13}C nuclei with 0, 1, 2 or 3 directly attached protons. The pulse sequence is the same as in Figures 8-9 and 8-10, but here only one special case, $\tau = [J(C,H)]^{-1}$, is considered. The vector diagrams a to e show the starting situation and the evolution of the magnetization vectors for quaternary, CH, CH_2 and CH_3 carbon nuclei. Acquisition of the second half of the echo followed by Fourier transformation gives the signals shown (schematically) on the right.

The effect of pulse field gradients on transverse magnetization:

In high-resolution NMR, the magnetic field Bo should be as homogenous as possible because small field variations ΔBo causes undesirable peak broadening (e.g. bad shimming).

However, introducing field inhomogeneity by linear pulse field gradients can be very useful for removing remaining magnetization in the x-y plane:

- **between FIDs**
- **within a pulse sequence for phase cycling**
- **within a pulse sequence for water suppression**
- **within a pulse sequence to measure diffusion constants**

A) Nuclei within different volume slices experience different effective field strengths:

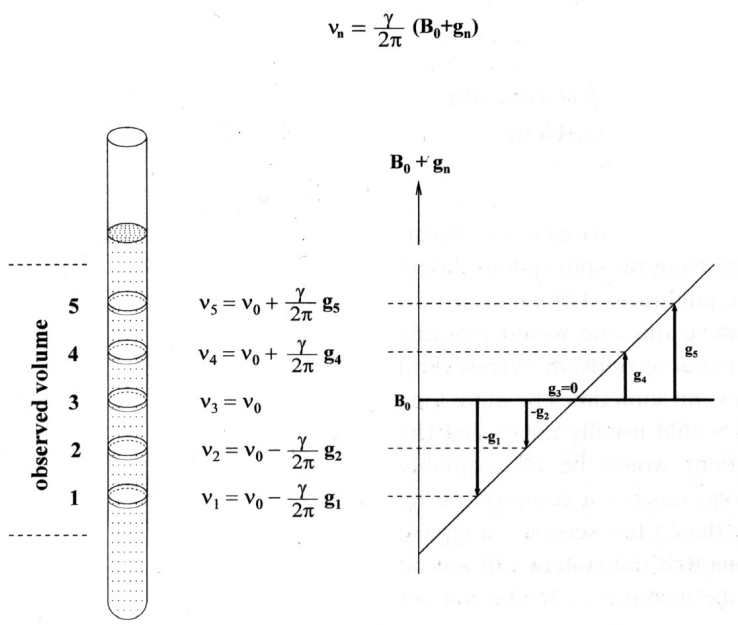

Figure 8-5.
Effect of applying a linear field gradient along the direction of the field B_0 (the z-direction). The quantities g_n are the contributions of the field gradient to the field B_0. ν_1 to ν_5 are the resonance frequencies for the five arbitrarily chosen slices 1 to 5. In the center of the observed sample (slice 3 in the example shown) g_n is zero, while it is positive above the center and negative below it.

B) A single gradient dephases magnetization in the x-y plane:

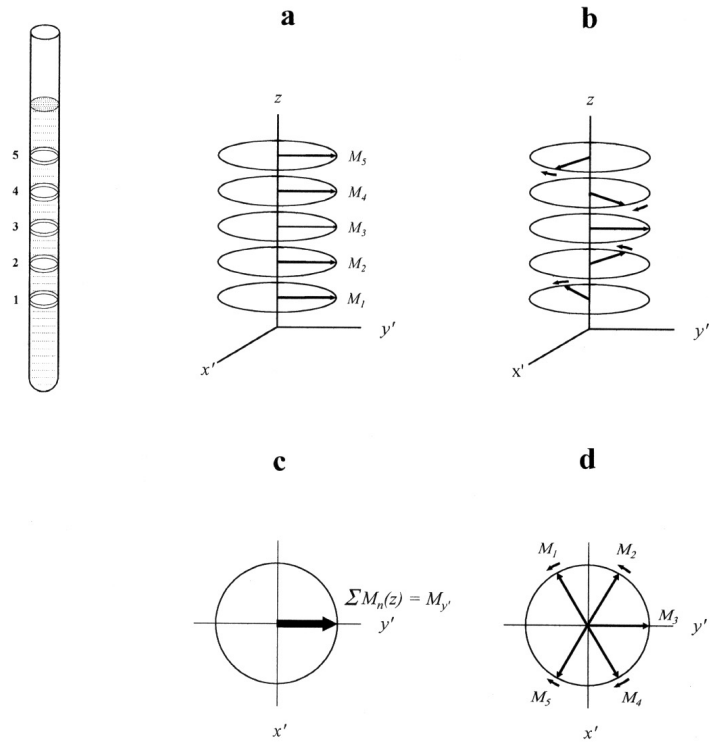

Figure 8-6.
The behavior of the transverse magnetization under the influence of a field gradient. As in Figure 8-5, five slices are shown, the gradient field contribution g_3 in slice 3 at the center of the observed volume being zero. A $90^\circ_{x'}$ pulse establishes the transverse magnetization vectors $\boldsymbol{M}_1$ to $\boldsymbol{M}_5$. Owing to the field gradient contributions g_1 to g_5 these precess with different frequencies ν_1 to ν_5. $\boldsymbol{M}_3$ remains along the y'-direction in the rotating frame, since both the magnetization and the frame have the same frequency ν_0, while the other transverse magnetization vectors rotate in the directions indicated by the small arrows (diagrams b and d). As a result of the fanning-out process the macroscopic transverse magnetization $\boldsymbol{M}_{y'}$ for the sample as a whole (diagram d) eventually falls to zero.

C) Phase coherence is regained by a second gradient applied in opposite direction

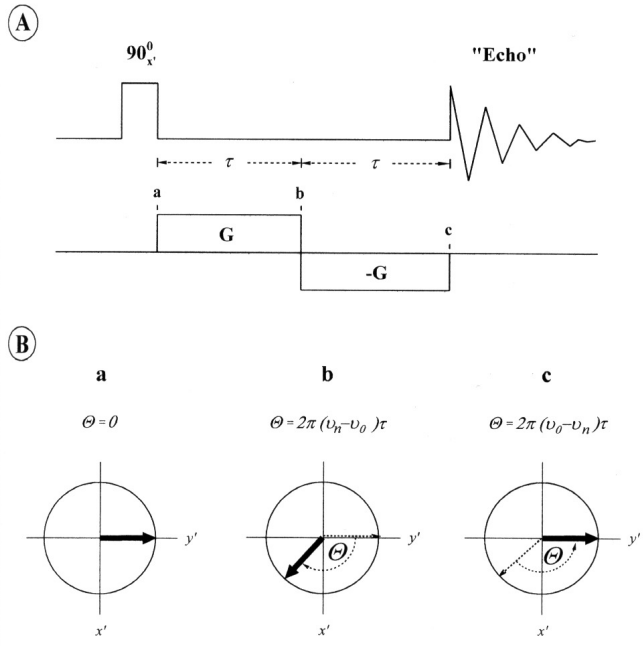

Figure 8-7.
The gradient echo experiment.
A: Pulse sequence. After the $90^\circ_{x'}$ pulse the field gradient G is applied for a time τ. A gradient of the same magnitude and duration is then applied in the opposite direction $(-G)$.
B: The vector diagrams show the behavior of the transverse magnetization for slice n. During the first interval τ, under the influence of the gradient G, it precesses through an angle Θ in the rotating frame (diagram b). During the second interval τ the process is reversed by the gradient $-G$, so that the transverse magnetization vector is again along the y'-direction, producing an echo.

The pulsed field gradient spin-echo experiment:

As for the standard spin-echo experiment, it refocuses

- **chemical shift**
- **Heteronuclear J coupling**
- **magnetic field inhomogeneity**

For simplification, lets consider a single ^1H on resonance, in the absence of heteronuclear J coupling, and no magnetic field inhomogeneity:

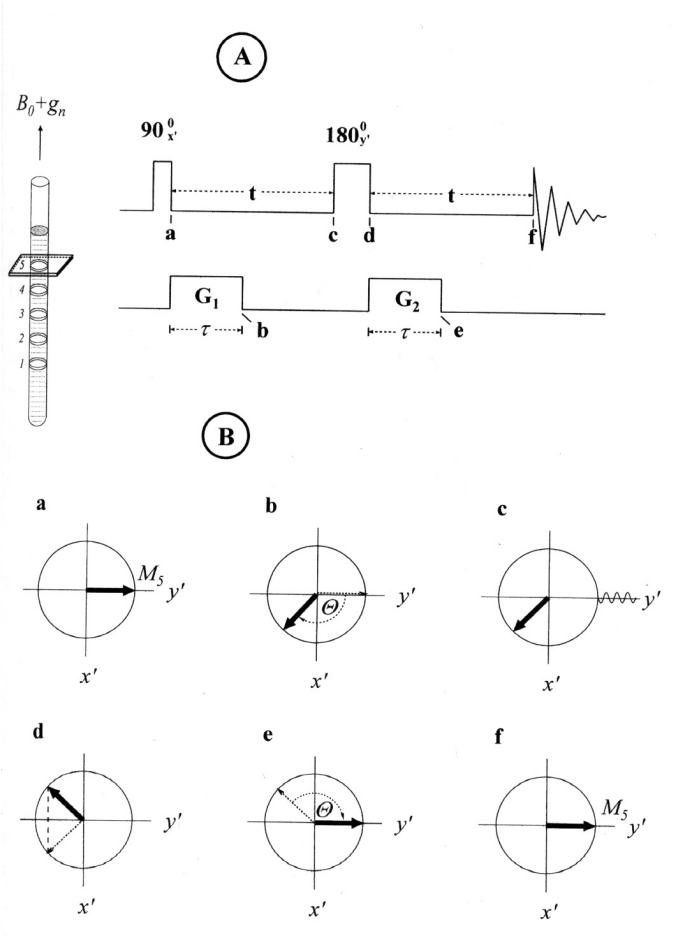

Figure 8-13.
The spin–echo experiment with pulsed gradient.
A: Spin–echo pulse sequence with the addition of a gradient field G_1 after the $90^\circ_{x'}$ pulse and a second (identical) gradient field G_2 after the $180^\circ_{y'}$ pulse.
B: The vector diagrams show the state of the transverse magnetization M_5 of slice 5 at each of the instants a to f in diagram A.

Axial diffusion means that the value of g_n, and therefore the precession frequency ν_n changes between the first and the second pulse field gradients. In this case, refocusing is incomplete and the intensity of the signal is reduced.

This effect can be used to measure <u>diffusion coefficients</u> and for <u>water suppression</u> in macromolecular NMR.